Hearing Research, 46 (1990) 41–52
Elsevier

HEARES 01369

Rate fluctuations and fractional power-law noise recorded from cells in the lower auditory pathway of the cat

Malvin C. Teich [1], Don H. Johnson [2], Anand R. Kumar [2] and Robert G. Turcott [3]

[1] *Departments of Electrical Engineering and Otolaryngology, Columbia University, New York, New York,*
[2] *Department of Electrical and Computer Engineering, Rice University, Houston, Texas, and* [3] *Center for Telecommunications Research, Department of Electrical Engineering, Columbia University, New York, New York, U.S.A.*

(Received 21 August 1989; accepted 30 December 1989)

The noise properties of the sequence of action potentials recorded from adult-cat auditory nerve fibers and lateral superior olivary units have been investigated under various stimulus conditions. Large fluctuations exhibited by the spike rate, and spike clusters evident in the pulse-number distribution, both indicate an unusual underlying sequence of neural events. We present results demonstrating that (i) the firing rate calculated with different averaging times can exhibit self-similar behavior; (ii) the pulse-number distribution remains irregular even for large numbers of samples; (iii) the spike-number variance-to-mean ratio increases with the counting time T in fractional power-law fashion for sufficiently large T; and (iv) the exponent in the power law generally depends on the stimulus level. The results obtained in our laboratories support the notion that all auditory-nerve and LSO units exhibit fractal neural firing patterns, as indicated earlier by Teich (IEEE Trans. Biomed. Eng. 36, 150–160, 1989).

Rate function; Pulse-number distribution; Fractal neural events; Auditory nerve; Lateral superior olive

Introduction

Experimental and theoretical evidence that the auditory neural spike train has a fractal character has recently been set forth by Teich (1988, 1989). Stationary fractal patterns can arise in the context of random systems or in systems exhibiting deterministic chaos. Fractal patterns exhibit order within apparent randomness, and reveal the presence of multiple scales of time and/or space.

In this paper we report further measurements relating to the noise properties of the sequence of action potentials recorded from barbiturate-anesthetized adult-cat primary auditory nerve fibers and lateral superior olivary (LSO) units. Standard extracellular microelectrode recording techniques were used (Kiang, Watanabe, Thomas, and Clark, 1965; Teich and Khanna, 1985; Tsuchitani and Johnson, 1985). The large fluctuations exhibited by the spike rate (Kumar and Johnson, 1984; Johnson and Kumar, 1985), and the spike clusters evident in the pulse-number distributions (Teich and Khanna, 1982, 1983, 1985; Teich and Turcott, 1988), are both indicative of an underlying fractal sequence of neural events (Teich, 1988, 1989).

We present results demonstrating that (i) the firing rate calculated with different averaging times can exhibit self-similar behavior; (ii) the pulse-number distribution remains irregular even for large numbers of samples; (iii) the spike-number variance-to-mean ratio increases with the counting time T in fractional power-law fashion for sufficiently large T; and (iv) the exponent in the power law generally depends on stimulus level.

The results presented in this paper are representative; all of the VIII-nerve and LSO units that we have studied to date behave in this manner. To this point, we have investigated 25 high-frequency units with spontaneous firing rates (for VIII-nerve units) ranging from 17 to 74 spikes/s. The measurements were carried out at three different

Correspondence to: M.C. Teich, Department of Electrical Engineering, Columbia University, New York, N.Y. 10027, U.S.A.

laboratories: Columbia University, University of Texas Health Science Center-Rice University, and MIT-Massachusetts Eye and Ear Infirmary Eaton-Peabody Laboratory of Auditory Physiology. They confirm that all auditory nerve fibers and LSO units examined to date show fractal neural firing patterns for sufficiently large observation times. A preliminary version of this work was presented at the 1989 Annual Meeting of the Association for Research in Otolaryngology (Teich, Johnson, and Kumar, 1989).

Results

Self-similarity of the firing rate

In Fig. 1(a), we illustrate the spontaneous firing rate of an auditory nerve fiber (Unit A), which has a characteristic frequency (CF) = 10.2 kHz. Two different time windows were used to compute the rate: T = 0.5 s (solid curve) and T = 5.0 s (dashed curve). The total time duration of the solid curve is 15 s (30 consecutive time windows, each of 0.5 s) whereas the total time duration of the dashed curve is 150 s (30 consecutive time windows, each of 5.0 s). Increasing the averaging time by a factor of 10 slightly reduces the magnitude of the fluctuations.

The firing rate of a simulated point process is illustrated in Fig. 1(b). The rate of events and the time windows were chosen to be the same as those for the auditory data shown in Fig. 1(a). These curves were constructed from a computer simulated dead-time-modified Poisson point process (DTMP) with a fixed nonparalyzable dead time $\tau_d = 2.95$ ms (Cox, 1962; Müller, 1974; Johnson and Swami, 1983; Prucnal and Teich, 1983). The choice of this particular value of τ_d is explained subsequently. In contrast to the auditory neural data, the T = 5.0 s computer data (dashed curve) exhibits substantially smaller fluctuations than does the T = 0.5 s computer data (solid curve).

The contrast is even more dramatic in the case of driven activity, as illustrated in Fig. 2(a). Firing rate data are shown for the same unit as illustrated in Fig. 1(a), but now with continuous-tone stimulation at the CF. The rate is generally higher than that in Fig. 1(a) because the unit is driven. Three different time windows are used to compute the rate: T = 0.5 s (solid curve), T = 5.0 s (dashed curve), and T = 50 s (dotted curve). The total time duration of the solid curve is 15 s (30 consecutive time windows, each of 0.5 s), the total time duration of the dashed curve is 150 s (30 consecutive time windows, each of 5.0 s), and the total time duration of the dotted curve is 550 s (11 consecutive time windows, each of 50 s). To minimize the effects of nonstationarity arising from adaptation, the first 250 s of driven data were ignored in the presentation provided in Fig. 2(a). The fluctuations of the rate do not appear to be smoothed under a change of time scale as large as 100, so that the process may be said to be self-similar (Mandelbrot, 1982; Teich, 1989).

The firing rate of a simulated dead-time-modified Poisson point process with the same rate, but now with a dead time $\tau_d = 2.48$ ms, is illustrated in Fig. 2(b) for comparison. The time windows are the same as those for the auditory data shown in Fig. 2(a). The substantial smoothing of the rate fluctuations with increasing counting time is in dramatic contrast to the self-similar behavior evidenced by the auditory data.

The degree to which the firing rate λ_T may be considered to be self-similar is quantitatively established by the dependence of its standard deviation σ_λ on the time window T. As elucidated in the Conclusion [see Eq. (3)], this relationship takes the form of a power law for sufficiently large time windows; the fractal dimension of the process α appears in the exponent.

Irregular nature of the pulse-number distribution

Another measure of the underlying neural firing pattern is the pulse-number distribution (PND). It is the probability of observing N spikes in the observation time T, versus the number of spikes N. The advantages to be gained by using this measure have been discussed in detail previously (Teich and Khanna, 1985; Teich and Turcott, 1988; Teich, 1989).

The PND was first used by Teich and Khanna (1982) as a measure of the sequence of primary auditory nerve fiber action potentials. The initial experiments were performed using a short counting time of T = 51.2 ms (Teich and Khanna, 1982, 1983, 1985). Most PND studies carried out in the auditory nerve since then have used counting times shorter than 50 ms (Westerman and Smith, 1984;

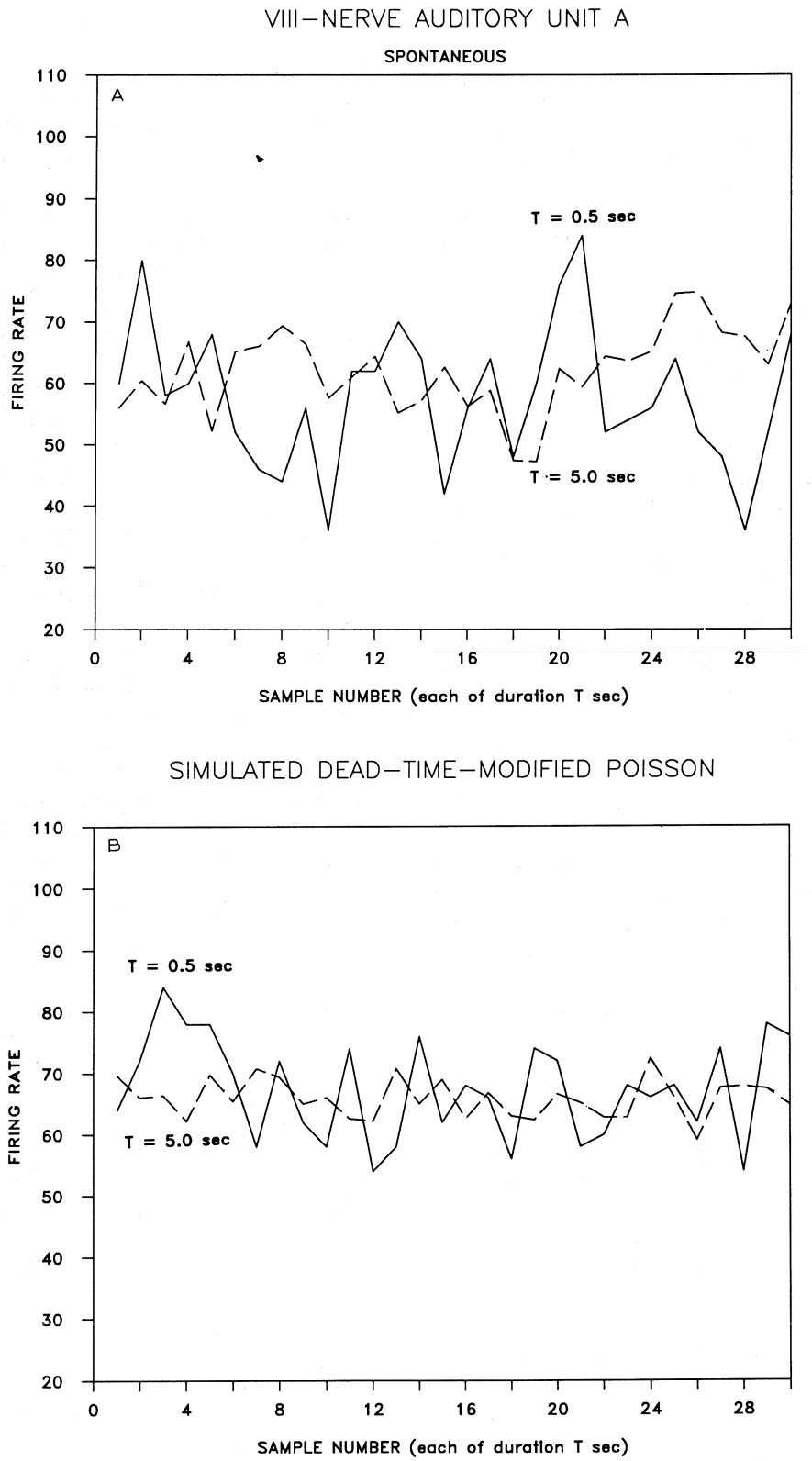

Fig. 1. (a) Spontaneous firing rate of an auditory nerve fiber (Unit A, CF = 10.2 kHz). Two different time windows are used to compute the rate: T = 0.5 s (solid curve) and T = 5.0 s (dashed curve). (b) The firing rate of a simulated dead-time-modified Poisson (DTMP) point process. The T = 5.0 s computer data (dashed curve) exhibits substantially smaller fluctuations than does the T = 0.5 s computer data (solid curve).

VIII—NERVE AUDITORY UNIT A

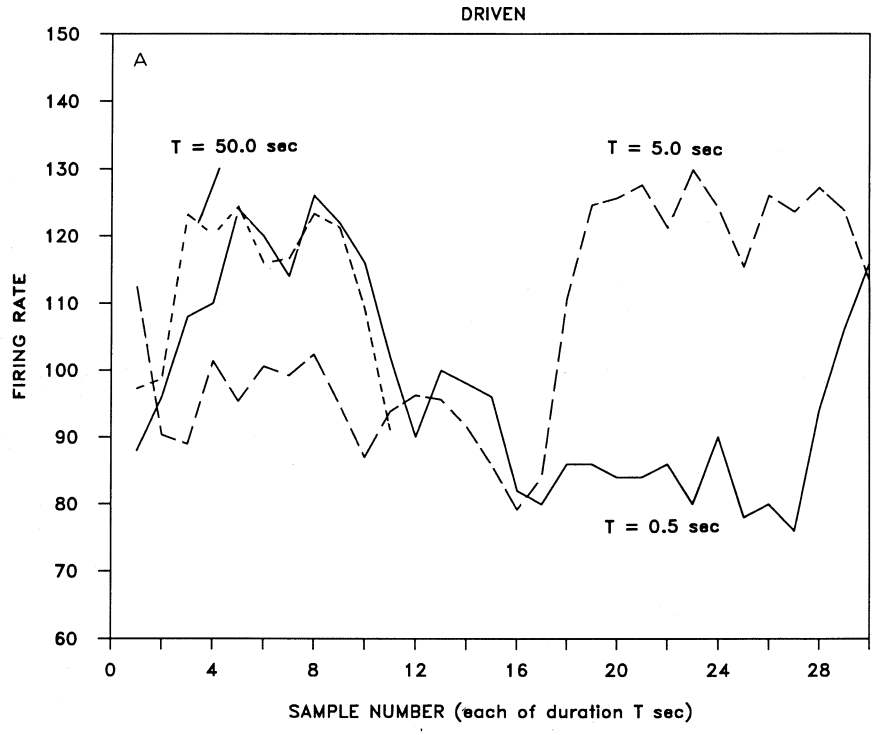

SIMULATED DEAD—TIME—MODIFIED POISSON

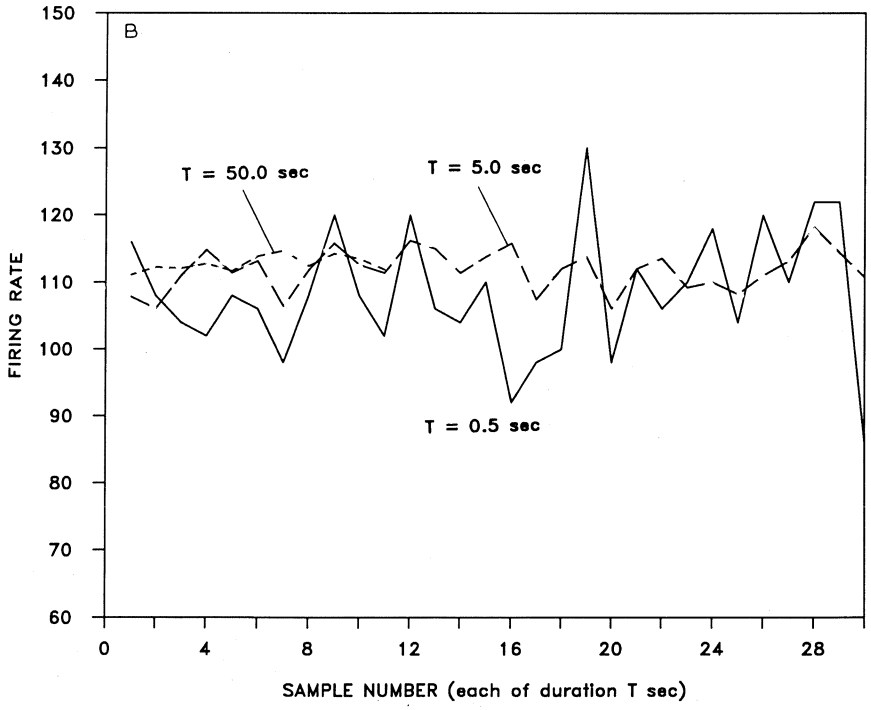

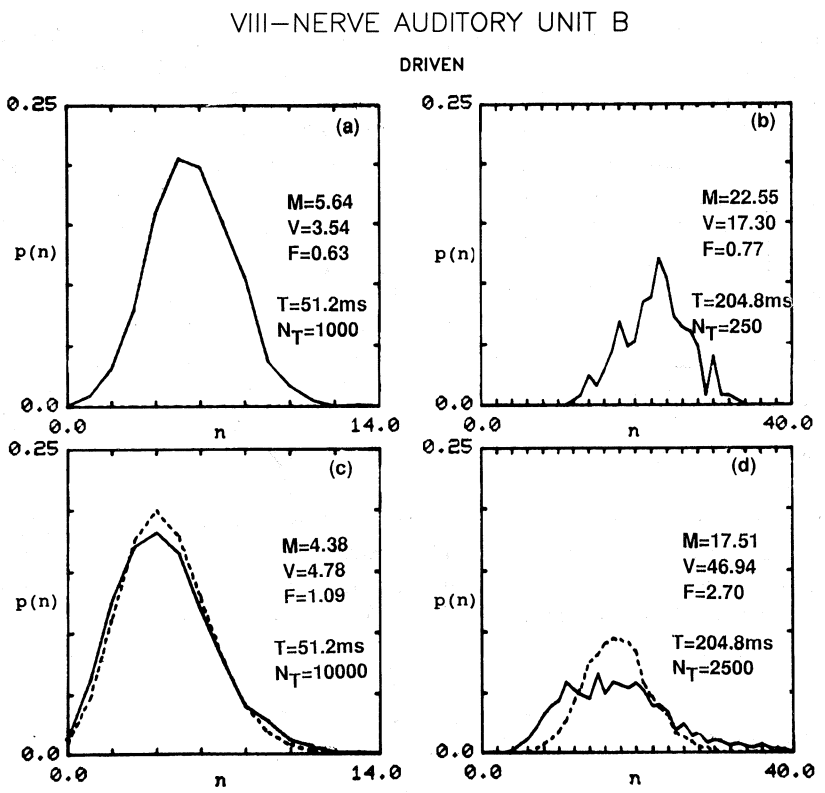

Fig. 3. PNDs for a high-spontaneous, high-frequency primary fiber (Unit B, CF = 12695 Hz, threshold = 41 dB SPL) stimulated by a pure tone at 61 dB SPL. The PND is the probability P (N,T) of observing N spikes in the observation time T, versus the number of spikes N. In all panels, each tic mark along the abscissa represents 2 spikes. Experimental values for the PND count mean M, count variance V, and variance-to-mean ratio F are specified in each of the panels. (a) T = 51.2-ms PND collected with $N_T = 1000$ samples (L = 51.2 s). (b) T = 204.8-ms PND constructed from the identical spike train as used in (a) so that $N_T = 250$ samples. (c) T = 51.2-ms PND collected with $N_T = 10000$ samples and therefore L = 512 s (solid curve); simulated-Poisson distribution with the same mean and same N_T (dotted curve). (d) T = 204.8-ms PND constructed from the identical spike train as used in (c) so that $N_T = 2500$ samples (solid curve); simulated-Poisson distribution with same mean and same N_T (dotted curve). As a result of the fractal nature of the spike train, the T = 204.8-ms PNDs remain irregular even when a large number of samples N_T is used. (After M. C. Teich, IEEE Trans. Biomed. Eng. 36, 150–160, 1989.)

Westerman, 1985; Relkin and Pelli, 1987). Some experimenters collected full auditory-nerve PNDs, but concentrated principally on their mean and variance (Young and Barta, 1986; Delgutte, 1987).

The unusual behavior of the PND for counting times longer than about 100 ms reveals a great deal about the character of the underlying neural spike train. PNDs with strikingly different char-

Fig. 2. (A) Firing rate of an auditory nerve fiber (Unit A, same unit shown in Fig. 1) driven by a continuous tone at the CF. Three time windows are used to compute the rate: T = 0.5 s (solid curve), T = 5.0 s (dashed curve), and T = 50 s (dotted curve). Increasing the averaging time by a factor of 100 does not decrease the magnitude of the fluctuations; the continuous-tone-driven process is self-similar. (B) The firing rate of a simulated dead-time-modified Poisson point process with the same time windows as in (a). The smoothing of the rate fluctuations with increasing counting time is in dramatic contrast to the self-similar behavior observed in the auditory data.

acteristics emerge from a given set of auditory spike data when the counting time T is increased above this value (Teich and Khanna, 1983; Teich and Turcott, 1988; Teich, 1989). An example is provided in Fig. 3 where several PNDs for a high-spontaneous, high-frequency primary auditory fiber (Unit B, CF = 12695 Hz, threshold = 41 dB SPL) are shown. The stimulus was a pure tone at 61 dB SPL (sound pressure level). The T = 51.2-ms PND collected with $N_T = 1000$ samples (experimental duration L = 51.2 s) is shown in (a). The PND in (b) is constructed from the identical set of spikes, but with T = 204.8-ms and $N_T = 250$ samples (L = 51.2 s). They clearly differ in character.

The solid curve in Fig. 3(c) represents the T = 51.2-ms PND collected with $N_T = 10000$ samples (L = 512 s) whereas the dotted curve is a simulated-Poisson distribution with the same mean and same N_T. Finally, the solid-curve PND in (d) is constructed from the identical set of spikes as the solid-curve PND in (c), but with T = 204.8 ms and $N_T = 2500$ samples (L = 512 s). The dotted curve in (d) is a simulated-Poisson distribution with the same mean and same N_T as the solid curve in (d). Experimental values for the PND count mean M, count variance V, and variance-to-mean ratio F are specified in each of the panels. The dotted curves have $F \approx 1$ inasmuch as they are both simulated Poisson distributions.

The difference between the T = 51.2-ms experimental PND [solid curve in Fig. 3(c)] and the T = 204.8-ms experimental PND [solid curve in Fig. 3(d)] is dramatic. The T = 204.8-ms PNDs remain irregular even when a large number of samples N_T is used. It is clear that the PND in Fig. 3(d) is far more jagged than the PND in Fig. 3(a), even though it is constructed from two-and-

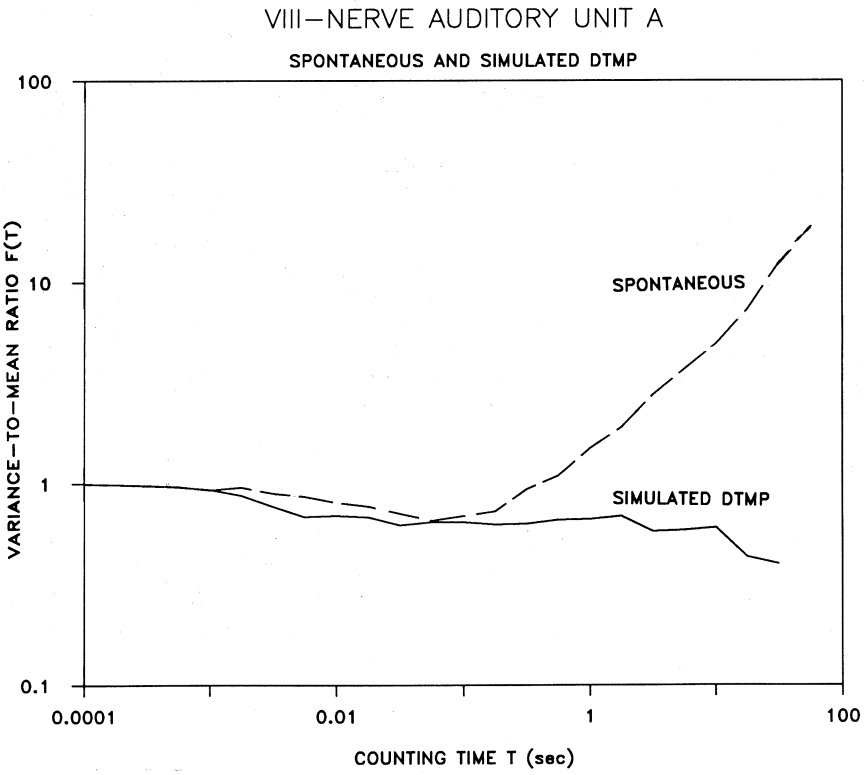

Fig. 4. Fano-time curve for spontaneous firing of a primary auditory fiber (Unit A) in an experiment of duration L = 400 s (dashed curve). Spontaneous rate fluctuations for this unit are displayed in Fig. 1(a). The Fano-time curve assumes a value of unity at short counting times, dips below unity for counting times > 1 ms, and finally increases in pure power-law fashion when the counting time exceeds about 400 ms. In contrast, the Fano-time curve for a simulated fixed-dead-time-modified Poisson process (solid curve) remains approximately constant (below unity) for all values of T larger than the dead time. The Fano-time curve for a Poisson process in the absence of dead time is always precisely unity.

a-half times as many samples. This phenomenon can be understood in the context of a fractal auditory neural spike train (Teich, 1989; Teich and Turcott, 1988).

Power-law growth of the Fano-time curve

The count variance-to-mean ratio is a useful measure of the PND in compact form. This ratio is often referred to as the 'Fano factor' since it was first used by Fano (1947) as a measure of the statistical fluctuations of the ionic number generated by individual fast charged particles. The Fano factor is a measure of the distribution as a whole, and carries different information than the individual probabilities comprised by the PND.

The Fano factor F(T), as a function of the counting time T, is shown in Fig. 4 for Unit A. This is the same auditory nerve fiber shown in Figs. 1(a) and 2(a). The results for spontaneous firings (dashed curve) were observed in an experiment of duration L = 400 s. The Fano-time curve is seen to assume a value of unity at short counting times, dip below unity for counting times above about 1 ms (where refractoriness comes into play), and finally to increase in power-law fashion (with an exponent of 0.6 for this unit) when the counting time exceeds about 400 ms. The fractal nature of the process manifests itself in this regime (Teich, 1989). All auditory nerve fibers examined to date exhibit this characteristic shape. For spontaneous firing, F typically assumes a minimum value ($0.6 \lesssim F_{min} \lesssim 0.9$) for counting times in the tens of ms. The onset of pure power-law behavior (with exponents in the range between 0.4 and 0.9), occurs at counting times between about 0.1 and 1.0 s.

The Fano-time curve for a simulated fixed-dead-time-modified Poisson process is shown for comparison (solid curve). As expected, it assumes a value of unity when $T \ll \tau_d$, dips below unity

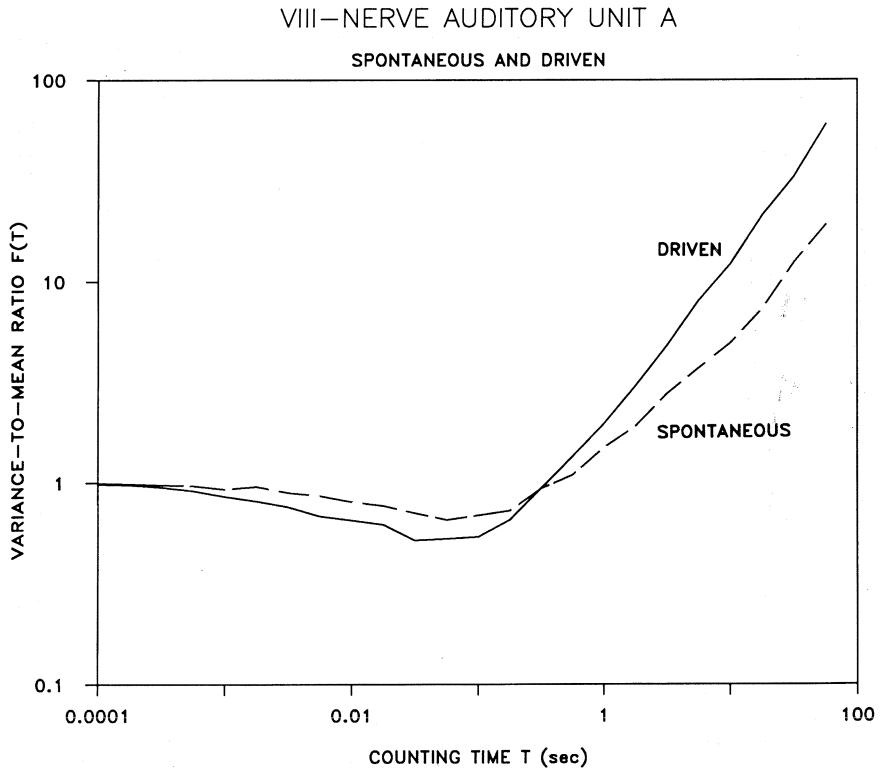

Fig. 5. Fano-time curve for continuous-tone-driven firing of Unit A in an experiment of duration L = 800 s (solid curve). The Fano-time curve for the spontaneous firing of this unit, which is shown in Fig. 4, is repeated here for purposes of comparison (dashed curve). Driven rate fluctuations for this unit are displayed in Fig. 2(a). The shapes of the Fano-time curves are similar for the spontaneous and driven firing; however the power-law exponent increases from 0.6 for the spontaneous firing to 0.8 for the driven firing.

when the counting time T approaches $\tau_d = 2.95$ ms, and remains approximately constant (below unity) for all values of T larger than τ_d (Müller, 1974; Teich, Saleh, and Peřina, 1984). The asymptotic theoretical value assumed by the DTMP Fano factor F_d is (Teich, 1985)

$$F_d \approx (1 - \lambda\tau_d)^2, \quad (1)$$

where λ represents the post-dead-time firing rate. Poisson processes modified by stochastic or relative dead time (Teich, Matin, and Cantor, 1978; Teich and Diament, 1980; Young and Barta, 1986) lead to Fano-time curves similar to those for fixed dead time. The dead-time simulations exhibited in Figs. 4, 1(b), and 2(b) make use of values of τ_d that satisfy Eq. (1) when the experimental value of λ and the minimum observed value of F are used.

Alteration of the firing pattern engendered by stimulation

The variance-to-mean ratio vs counting time T for this same auditory nerve fiber (Unit A) is shown in Fig. 5 for driven activity with a continuous tone at the CF (solid curve), collected for L = 800 s. The spontaneous data shown in Fig. 4 are repeated for comparison (dashed curve). Although the shapes of the Fano-time curves are similar in both cases, the minimum value for the Fano factor is lower under stimulation (dead time has a greater effect on F when the rate is higher), and the power-law exponent is greater (it increases from 0.6 to 0.8 when the tone is applied). This represents an increase in the fractal dimension, indicating that the stimulus not only alters the rate of firing but the pattern of firing as well (Teich, 1989). The presence of the stimulus produces a

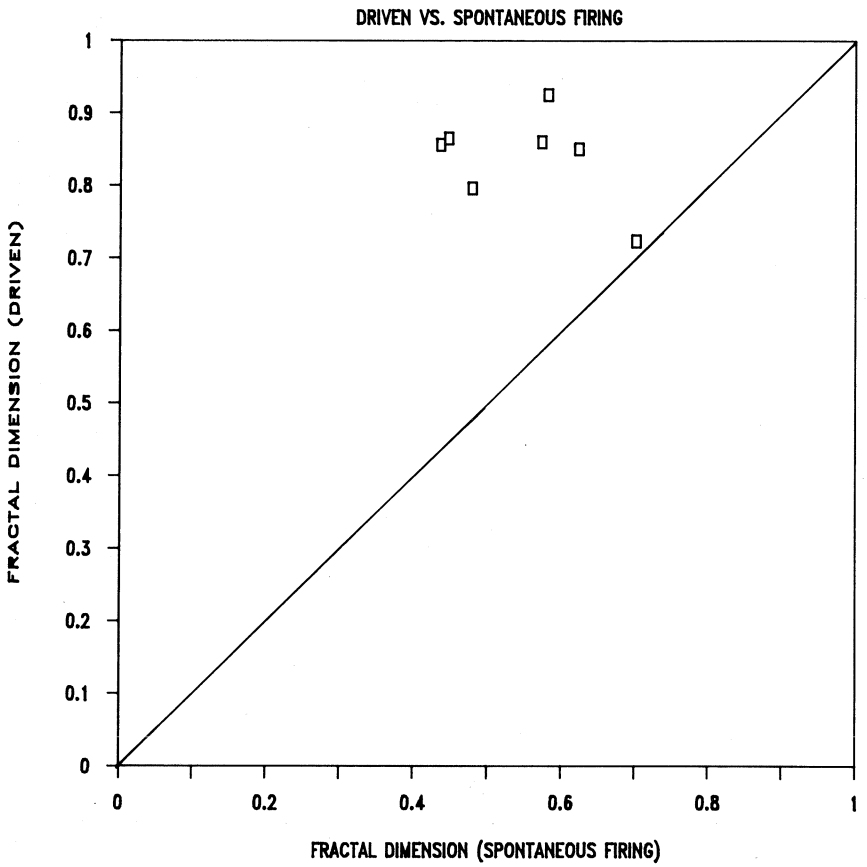

Fig. 6. Relationship of the power-law exponents for several auditory-nerve units, under conditions of driven and spontaneous firing. The exponent, which represents the fractal dimension of the process, generally increases under continuous-tone stimulation.

more clustered point process and, therefore, larger rate fluctuations.

For driven firing, F typically assumes a minimum value ($0.5 \lesssim F_{min} \lesssim 0.9$) for counting times in the tens of ms. The onset of pure power-law behavior (with exponents in the range between 0.6 and 1.0), occurs at counting times between about 0.1 and 0.5 s. The relationship of the power-law exponents for several primary auditory units, under conditions of driven and spontaneous firing, is demonstrated in Fig. 6. For auditory nerve fibers, the exponent representing the fractal dimension generally increases in the presence of continuous-tone stimulation.

Fano-time curves for units in the lateral superior olive

The Fano-time curve for a continuous-tone-driven fast-chopper cell in the LSO (Unit C) is shown in Fig. 7. This high-frequency unit (CF = 15 kHz) exhibited a mean firing rate of ≈ 120 spikes/s when stimulated monaurally (at the CF) by a pure tone at a level of 30 dB SPL above threshold. The overall duration of the experimental data set used to generate Fig. 7 was L = 375 s; to minimize the effects of nonstationarity arising from adaptation, the first 200 s of the full 575 s data set were ignored.

As with auditory nerve fibers (or indeed any refractoriness-modified firing pattern), the LSO Fano-time curve assumes a value of unity at sufficiently short counting times. These curves generally reach their minimum Fano factor (typically $0.3 \lesssim F_{min} \lesssim 0.9$) for counting times in the tens of ms. The dip in the Fano-time curve is more dramatic than that for primary fibers (compare with Fig. 5), in accordance with the observation that LSO firing patterns are more regular over the term of tens of ms. For sufficiently long counting times (between 0.1 s and 1.0 s), the Fano factor

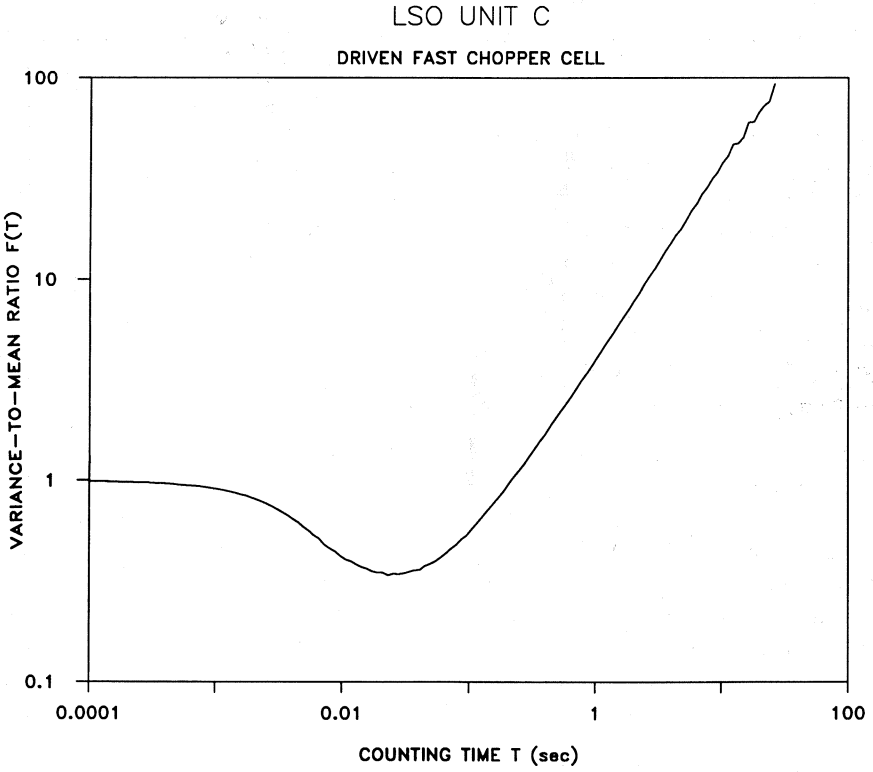

Fig. 7. Fano-time curve for a continuous-tone-driven fast-chopper cell (Unit C) in the lateral superior olivary complex (LSO). This high-frequency unit (CF = 15 kHz) exhibits a mean firing rate of ≈ 120 spikes/s when stimulated monaurally (at the CF) by a pure tone at a level of 30 dB SPL above threshold. The overall shape of the curve is similar to those exhibited by primary fibers, although the dip is more dramatic (compare with Fig. 5). For sufficiently long counting times, the Fano factor climbs in the same characteristic power-law fashion as observed for auditory units. All LSO units examined to data exhibit this characteristic shape.

exceeds unity and climbs in the same characteristic power-law fashion as observed for auditory units. The power-law exponent for Unit C is 0.9; most often it lies in the range between 0.7 and 1.0 for LSO units, which is not unlike the range observed for driven primary auditory fibers. A comparison between spontaneous and stimulated firing, such as that illustrated in Fig. 5 for primary auditory units, is not possible since LSO units fire only in the presence of an acoustic stimulus. All LSO units examined to date exhibit this characteristic shape.

Conclusion

The spike trains observed from VIIIth-nerve fibers and LSO units exhibit unusual characteristics. They manifest highly irregular rates, irregularly shaped pulse-number distributions (even when the number of samples is large), fractional power-law behavior in the Fano-time curve, and a fractional power-law exponent that appears to depend on the level of stimulation.

It is of interest to note that cochlear-nucleus (CN) PNDs, recently reported by Shofner and Dye (1989) using a counting time of $T = 400$ ms, behave similarly to those observed in primary fibers and LSO units. Thus, the sequence of action potentials at three distinct loci in the auditory pathway (VIII-th nerve, LSO, and CN) appear to behave similarly; all exhibit fractal neural firing patterns for sufficiently large observation times (Teich, 1989).

One consequence of fractal neural activity is the relatively slow convergence achieved by time averaging, as is evident from Figs. 1(a) and 2(a). The dependence of the standard deviation σ_λ of the rate λ_T on the averaging time T may be quantitatively determined from the fractal dimension. Using the relation $\lambda_T = n/T$, where n is the random number of neural spikes in the time T, it is clear that the expression for the variance of the firing rate is $\mathrm{Var}(\lambda_T) = (1/T^2)\mathrm{Var}(n)$. By definition, $\mathrm{Var}(n) = \bar{n}F(T)$, where $\bar{n}$ is the mean number of events in the time T, so that $\mathrm{Var}(\lambda_T) = (1/T^2)\bar{n}F(T)$. Since $\bar{n} \propto T$ and, for sufficiently large T, $F(T) \propto T^\alpha$, where α is the power-law exponent (fractal dimension) of the Fano-time curve, we obtain

$$\mathrm{Var}(\lambda_T) \propto 1/T^{1-\alpha}. \tag{2}$$

The standard deviation of the rate is therefore given by

$$\sigma_\lambda \propto 1/T^{(1-\alpha)/2}. \tag{3}$$

Non-fractal processes have a fractal dimension $\alpha = 0$ so that the standard deviation of the rate is proportional to $1/T^{\frac{1}{2}}$; thus the rate converges quickly with increased averaging. Processes with $\alpha \to 1$ have a standard deviation that is independent of T so there is no convergence with time averaging and the rate process is fully self-similar. Thus estimates of the mean rate converge more slowly with increasing T for fractal processes than for non-fractal processes, with the rate of convergence depending on the fractal dimension α. Furthermore, because the power-law exponent associated with driven activity in primary fibers is generally greater than that associated with spontaneous activity, as shown in Fig. 6, estimates of the mean rate for driven activity converge more slowly than do estimates for spontaneous activity. The implications of this observation for the extraction of loudness by more central portions of the auditory system are not known.

Fractal behavior is not manifested over short time scales, however, so that certain types of measurements (e.g., interspike interval histograms and post-stimulus time histograms) will not reveal this behavior. Point process models based on such measures will therefore be limited in their applicability, and find use only in the modeling of short-term effects. Indeed, the dead-time-modified Poisson process model has achieved its success in this domain; this model clearly cannot provide a proper characterization of the sequence of action potentials in the auditory system, at least at the three loci indicated above. Indeed, applying a stimulus to a primary auditory unit results in an alteration of the pattern of firing, as well as the rate of firing (Teich, 1989). The sequence of primary fiber action potentials becomes more clustered and the rate fluctuations become larger.

It is clear that a newer and more powerful point process model is required to account for the

more complete measurements now available. Several fractal point process models present themselves as plausible candidates (Teich, 1989). The underlying fractal behavior of the neural spike train could originate at any of a number of loci. For example its origin might be in deterministic chaos, possibly associated with the nonlinear dynamics of the cellular vibrations in the Organ of Corti (Teich, Khanna, and Keilson, 1989). Alternatively, it might arise from a fractal stochastic process. One model that shows particular promise is the FSNDP; it is a doubly stochastic Poisson point process driven by fractal shot noise (Lowen and Teich, 1989a, 1989b; Teich, Turcott, and Lowen, 1990). The predictions offered by this model are in good agreement with a broad range of auditory neural-event data.

Acknowledgments

This work was supported by the National Institutes of Health and by the National Science Foundation. We are grateful to N. Y-S. Kiang for providing the data for auditory unit A and to C. Tsuchitani for providing the data for LSO unit C.

References

Cox, D.R. (1962) Renewal Theory, Methuen, London.

Delgutte, B. (1987) Peripheral auditory processing of speech information: Implications from a physiological study of intensity discrimination. In: M.E.H. Schouten (Ed.) The Psychophysics of Speech Perception, Nijhoff, Dordrecht, The Netherlands, pp. 333–353.

Fano, U. (1947) Ionization yield of radiations. II. The fluctuations of the number of ions. Phys. Rev. 72, 26–29.

Johnson, D.H. and Kumar, A. (1985) Analysis of the stationarity of models of auditory-nerve fiber discharge patterns. J. Acoust. Soc. Am. Suppl. 1 77, S93.

Johnson, D.H. and Swami, A. (1983) The transmission of signals by auditory-nerve fiber discharge patterns. J. Acoust. Soc. Am. 74, 493–501.

Kiang, N. Y-S., Watanabe, T., Thomas, E.C. and Clark, L.F. (1965) Discharge Patterns of Single Fibers in the Cat's Auditory Nerve. Research Monograph No. 35, MIT Press, Cambridge, MA.

Kumar, A. and Johnson, D.H. (1984) The applicability of stationary point process models to discharge patterns of single auditory-nerve fibers. Rice Univ. Dept. Elect. Eng. Tech. Rept. 84–09, Houston, TX.

Lowen, S.B. and Teich, M.C. (1989a) Generalised 1/f shot noise. Electronics Lett. 25, 1072–1074.

Lowen, S.B. and Teich, M.C. (1989b) Fractal shot noise. Phys. Rev. Lett. 63, 1755–1759.

Mandelbrot, B.B. (1982) The Fractal Geometry of Nature. W. H. Freeman, New York.

Müller, J.W. (1974) Some formulae for a dead-time-distorted Poisson process. Nucl. Instrum. Methods 117, 401–404.

Prucnal, P.R. and Teich, M.C. (1983) Refractory effects in neural counting processes with exponentially decaying rates. IEEE Trans. Syst. Man Cybern. SMC-13, 1028–1033.

Relkin, E.M. and Pelli, D.G. (1987) Probe tone thresholds in the auditory nerve measured by two-interval forced-choice procedures. J. Acoust. Soc. Am. 82, 1679–1691.

Shofner, W.P. and Dye, R.H., Jr. (1990) Statistical and receiver operating characteristic analysis of empirical spike count distributions: Quantifying the ability of cochlear nucleus units to signal intensity changes. J. Acoust. Soc. Am. 86, 2172–2184.

Teich, M.C. (1985) Normalizing transformations for dead-time-modified Poisson counting distributions. Biol. Cybern. 53, 121–124.

Teich, M.C. (1988) Fractal character of the auditory neural spike train. J. Acoust. Soc. Am. Suppl. 1 84, S55.

Teich, M.C. (1989) Fractal character of the auditory neural spike train. IEEE Trans. Biomed. Eng. 36, 150–160.

Teich, M.C. and Diament, P. (1980) Relative refractoriness in visual information processing. Biol. Cybern. 38, 187–191.

Teich, M.C. and Khanna, S.M. (1982) Pulse-number distribution for the neural discharge in the cat's auditory nerve. J. Acoust. Soc. Am. Suppl. 1 71, S17.

Teich, M.C. and Khanna, S.M. (1983) Behavior of the pulse-number distribution for the neural spike train in the cat's auditory nerve. J. Acoust. Soc. Am. Suppl. 1 74, S7.

Teich, M.C. and Khanna, S.M. (1985) Pulse-number distribution for the neural spike train in the cat's auditory nerve. J. Acoust. Soc. Am. 77, 1110–1128.

Teich, M.C. and Turcott, R.G. (1988) Multinomial pulse-number distributions for neural spikes in primary auditory fibers: Theory. Biol. Cybern. 59, 91–102.

Teich, M.C., Johnson, D.H. and Kumar, A. (1989) Spontaneous rate fluctuations and fractional power-law noise recorded from cat auditory nerve fibers. Abstr. Assoc. Res. Otolaryngol. No. 139, p. 123.

Teich, M.C., Khanna, S.M. and Keilson, S.E. (1989) Nonlinear dynamics of cellular vibrations in the organ of Corti. Acta Otolaryngol. (Stockholm) Suppl. 467, 265–279.

Teich, M.C., Matin, L. and Cantor, B.I. (1978) Refractoriness in the maintained discharge of the cat's retinal ganglion cell. J. Opt. Soc. Am. 68, 386–402.

Teich, M.C., Saleh, B.E.A. and Peřina, J. (1984) Role of primary excitation statistics in the generation of anti-bunched and sub-Poisson light. J. Opt. Soc. Am. B 1, 366–389.

Teich, M.C., Turcott, R.G. and Lowen, S.B. (1990) Identification of the Point Process Characterizing the Auditory Neural Spike Train. Abstr. Assoc. Res. Otolaryngol. 155, 141.

Tsuchitani, C. and Johnson, D.A. (1985) The effects of ipsilateral tone burst stimulus level on the discharge patterns of

cat lateral superior olivary units. J. Acoust. Soc. Am. 77, 1484–1496.

Westerman, L.A. (1985) Adaptation and recovery of auditory nerve responses. Syracuse Univ. Inst. Sensory Research Tech. Rept. ISR–S–24, Syracuse, NY.

Westerman, L.A. and Smith, R.L. (1984) Adaptation and variability of spike discharge of auditory nerve. J. Acoust. Soc. Am. Suppl. 1 75, S13.

Young, E.D. and Barta, P.E. (1986) Rate responses of auditory nerve fibers to tones in noise near masked threshold. J. Acoust. Soc. Am. 79, 426–442.